14th IEA Heat Pump Conference
15-18 May 2023, Chicago, Illinois

Efficiency Improvement Of A High Capacity Transcritical CO_2 Heat Pump For Human Comfort In Large Buildings

Hakim Nesreddine[a], Dominique Monney[b*], Wayne Wehber[c]

[a]Hydro Quebec, 600 avenue de la Montagne, Shawinigan, QC G9N 7N5, Canada
[b] Emerson Commercial & Residential Solutions | 145 Sherwood Drive, Brantford, ON N3T 1N8, Canada
[c]Vilter Manufacturing LLC, 5555 S Packard Ave, Cudahy WI 53110-8904, USA

Abstract

Transcritical CO_2 heat pumps have the potential to be environmentally friendly to decarbonize buildings. This technology is very efficient for water heating applications. However, they generally exhibit poor efficiencies for space heating due to high return temperatures. This paper presents new experimental test data obtained by operating a single screw industrial heat pump for space heating and cooling in large buildings. This transcritical CO_2 pilot-scale prototype has a maximum heating and cooling thermal capacity of 1.35 and 1.05 MW, respectively. The results show that decoupling the thermal load from the CO_2 heat pump by the use of thermal storage tanks increases substantially the coefficient of performance (COP) of the system compared to the reference case (without heat storage and temperature conditioning).

Selection and/or peer-review under the responsibility of the organizers of the 14th IEA Heat Pump Conference 2023.

Keywords: Building; Heat pump; Transcritical CO_2; Pilot-scale prototype

1. Introduction

Heat pumps are increasingly recognized as an efficient and low-carbon energy technology for heating, cooling and sometimes for providing hot water to buildings. The global heat pump market has expanded rapidly over the last few years, with around 190 million units in operation in buildings worldwide in 2021, the three main markets being in China (33%), North America (23%) and Europe (12%) [1,2]. Though being considered as a key and cost-effective component towards the reduction of carbon emissions in the residential and commercial sectors, heat pumps currently provide only 10% of the global heating need in buildings. In the 2050 carbon neutrality scenario, the world heat pump stock should reach 600 million by 2030, representing 20% of the global heating needs and having a more preponderant position to face the increased cooling needs. Countries currently develop different strategies (constraining building codes and standards, performance-based labels, grants to support system's acquisition or privileged electricity tariff) to accelerate the deployment of heat pumps in residential and commercial buildings. Some markets also credit the heat supplied by heat pumps as renewable such that they get eligible to specific grants [1]. However, their market penetration remains relatively slow. Gaur et al. [3] discussed the main barriers to their integration: high upfront costs, uncertainty in policy, lack of standards, public acceptance and limitation of the electrical networks.

Heat pump technology allows to uplift low-grade temperature heat sources to a useful temperature level (sink) using electricity. Thus, they can operate using low-grade renewable energy sources (air, water, ground or solar), but also using waste heat. They can provide both heating and cooling (reversible heat pumps), separately or simultaneously, with no heat dissipation. They are then highly efficient with coefficients of performance (COP) typically ranging from 3 to 5 [4]. When the electricity used to drive the compressor comes from a renewable source (like hydroelectricity as it is the case in the Québec province for example), all the

*Corresponding author. Tel.: +1 514 946 1882
E-mail address: Dominique.Monney@Emerson.com

useful heat provided by the heat pump gets zero-carbon. Besides the prime objective of efficient decarbonation, heat pumps may also play a role to enhance the energy security of countries.

As shown by Gaur et al. [3], the literature on heat pumps is quite abundant and the number of publications continues to rise exponentially. The interested reader can refer to the recent review of Ni et al. [5] for more details about heat pump systems for heating and cooling of buildings. The authors focused on air and ground heat pumps integrating a thermal energy storage under the form of water, phase change materials or ground. Wang et al. [4] discussed the main parameters affecting the performance of heat pumps: hybridization of the different heat sources and sinks depending on the temperature levels, compressor efficiency and potential integration of a thermal energy storage.

There is no consensus on the appropriate definition of a large-scale heat pump. For the European Heat Pump Association (EHPA), heat pump is considered large if its capacity exceeds 100 kW. Their potential integration for district heating systems and their impact are constantly investigated through case studies mainly in North Europe : Baltic countries [6], Germany [7] or Denmark [8] among other examples. These different works enable to compare the benefit of heat pumps compared to other sources (biomass [6], coal-fired combined heat and power system [7], mixed sources [8]) but also demonstrate that results are strongly case-dependent. David et al. [9] analyzed the existing electricity-driven heat pumps with a thermal capacity output equal or greater to 1 MW installed in Europe. They highlighted the huge potential for using sewage water and ambient water as the main heat sources followed by geothermal energy. Ground source heat pumps are indeed preferred over air source ones in Nordic climates as they are more constant and at higher temperature levels. Schlosser et al. [10] reviewed the applications, performance, economic feasibility and industrial integration of large-scale heat pumps. Their analysis, which gathers 155 large-scale heat pumps, covered all types of refrigerants, compressors, heat sources, etc.

As already mentioned, compressor efficiency plays a crucial role on the system performance. Jesper et al. [11] analyzed a database of 33 large-scale heat pumps from 11 different manufacturers. The distribution between reciprocating piston, screw and scroll compressors was well balanced. Screw compressor-based heat pumps exhibited the highest lift temperature difference and the largest nominal thermal output range. Wang et al. [12] proposed a matching strategy for a screw compressor integrated in a heat pump. It consists in the matching of the built-in volume of the compressor and the annual heating and cooling demands. They also introduced a new performance index denoted ACOPA (Annual integrated Coefficient of Performance under Actual operating conditions). For a ground-source heat pump, they showed numerically that such a strategy may improve the ACOPA by 6%.

R134a and R245fa are certainly the most used refrigerants in large-scale heat pumps [10, 11]. Due to their progressive phase-out, new low Global Warming Potential (GWP) refrigerants have to be considered. Hydrocarbons like R600 (n-butane) or R601 (pentane) have a low GWP but are highly flammable such that their filling capacity is limited to 2.5 kg in heat pumps in Europe, excluding them from potential large-scale applications. The use of alternative natural refrigerants in large-scale heat pumps with a low GWP and a favourable safety classification like R718 (water) or R744 (carbon dioxide), though being highly attractive, is still not state-of-the-art technology according to Jesper et al. [11]. As shown recently by Song et al. [13], transcritical CO_2 heat pumps are widely considered for water heating in buildings or for industrial processes and attention is now turned more on their performance optimization by ejector or vortex tube. Their application for space heating is scarcer. Schlosser et al. [10] proposed a correlation for the COP of transcritical CO_2 heat pumps based on four series from the same manufacturer, all using a reciprocating piston compressor. It represents 936 operating points in total. COP does not depend on the logarithmic mean temperature on the heat sink but depends only on the lift temperature difference.

To fully benefit from the heat pump potential, thermal energy storage is deemed necessary to continuously operate the system, shift the heat production to off-peak hours and decrease the thermal capacity to less than the maximum heating requirement among other benefits. It results in reduced installation and operating costs. Osterman and Stritih [14] proposed a recent review on compression heat pump systems including thermal energy storage (TES) for heating and cooling in buildings. Energy can be stored under three different forms, namely sensible storage, latent storage and thermo-chemical heat storage. Sensible TES through water storage tanks are the more simple and common solution. The authors found that in most cases, air is used as a balancing source and the capacities of heat pumps and the size of storage tanks remains relatively small. No study concerned the experimental investigation of a ground source transcritical CO_2 large-scale heat pump coupled to a TES for space heating and cooling, as in the present work. Liu et al. [15] considered a water source CO_2 heat pump with TES but at a small scale: 3 kW of nominal thermal capacity and small water storage tanks (around 170 L each for the hot and cold tanks). Alkhwildi et al. [16] developed a numerical model based on TRNSYS of ground source heat pump with hybrid TES (water and salt-hydrate) used to reduce the peak electricity demand of a 180 m² house in Toronto, Canada. A 2.5 m³ water tank was found sufficient to fully shift load. The results are theoretical and difficult to reproduce as no details on the type of heat pump and refrigerant used are provided.

Scientific and technical innovation is still required to improve the performance and durability of heat pumps, enhance their flexibility for the heating and cooling of large buildings and accelerate their market penetration. To the best of the authors' knowledge, the present work is the first to demonstrate the potential of a single screw industrial transcritical CO_2 heat pump for space heating and cooling in large buildings at the pilot scale. The addition of a water storage tank having a thin thermocline separating its hot and cold sections drastically improves the performance of the system by enabling to decouple the thermal load from the heat pump. It also allows to feed the heat pump's evaporator when the heat source is insufficient, which has never been demonstrated at this scale for this particular heat pump.

The paper is organized as follows: the experimental set-up and the associated instrumentation are described in detail in Section 2. The results are presented in Section 3. The discussion focuses on the benefit of decoupling the thermal load from the heat pump cycle by adding a large capacity thermal storage tank. Conclusions and future views are finally provided in Section 4.

2. Prototype Description

The test rig of the water source transcritical CO_2 heat-pump consists of three major components: water-loop system, heat-pump system, and data collection system. The schematic diagram of this experimental system is shown in Figure 1. It is composed of a gas cooler, an evaporator, a compressor, a flash tank, an internal heat exchanger, and an electronic expansion valve (EEV). The water loop system includes thermal storage tanks that decouple the thermal load from the CO_2 heat pump and allow performance enhancements. Detailed information about the main components is summarized in Table 1.

Table 1. Main components.

Component	**Type**	**Characteristics**
Compressor	Open Single Screw	Displacement: 452 m³/h Maximum rotating speed: 4200 rpm Maximum operating pressure: 103.4 bar Maximum Motor capacity: 643 kW
Gas cooler	Shell & Tubes Heat Exchanger	Shell: ϕ323.85mm (CO_2) Tube (Nb: 138): ϕ 12.7 mm (Water)
Evaporator	Flooded Shell & Tubes Heat Exchanger	Shell: ϕ*609.6*mm (CO_2) Tubes (Nb: 360): ϕ *19.05* mm (Water)
Flash tank	Custom built	-
Expansion valves	Electronic	Opening: 0-100%
Internal heat exchanger	Copper brazed plates	-
Thermal storage tanks	Custom built	Total volume of 40,000 l[2]

T-type thermocouples were adopted to measure the temperatures in the experimental system. The measurement accuracy is ±0.2 °C in the range of −10 °C to 150 °C. CO_2 mass flowrate was measured by a Coriolis mass flowmeter with the accuracy at ±0.1% in the range of 26 to 9,072 kg/h. Pressure transmitters with the accuracy at ±0.25% (0–6 MPa and 0–16 MPa, respectively) were used to measure the CO_2 pressures. Turbine volumetric flowmeters with the accuracy at ±0.5% were used to measure water flowrates.

[2] The volume and geometry characteristics have been determined using CFD simulation.

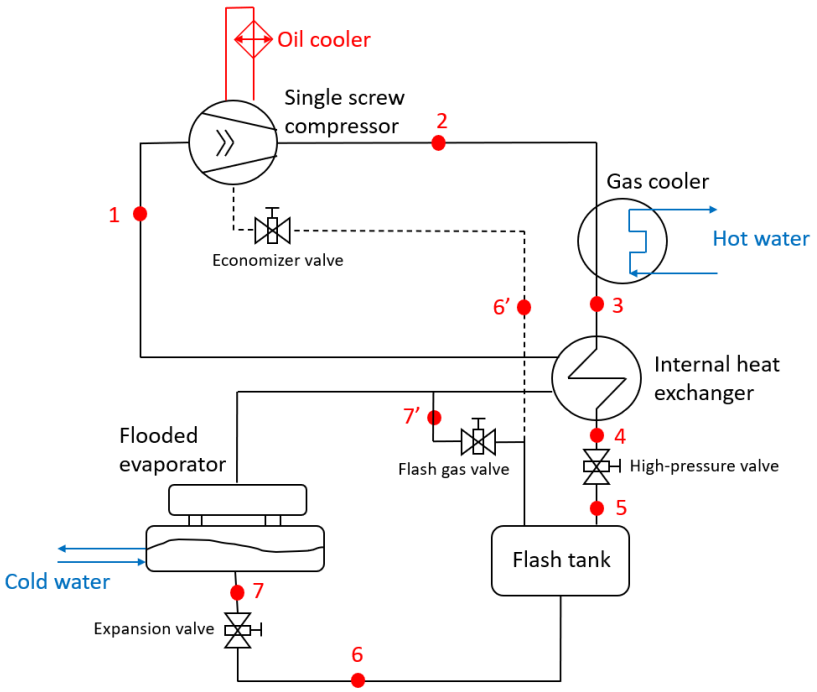

Fig. 1. Simplified configuration of transcritical CO_2 heat pump

Figure 2 shows the p-h diagram of the heat pump system under study. The main system cycle is 1-2-3-4-5-6-7-1. The refrigerant is compressed from point 1 (superheated vapour) to point 2 (supercritical fluid) by the compressor. The water is heated in the gas cooler by the heat released from point 2 to point 3. The water is cooled from point 7 to the gas saturation line by the CO_2 evaporation and CO2 is overheating from the saturation vapour line to point 1 by the heat absorbed in the internal heat exchanger. (Point 3 to 4)

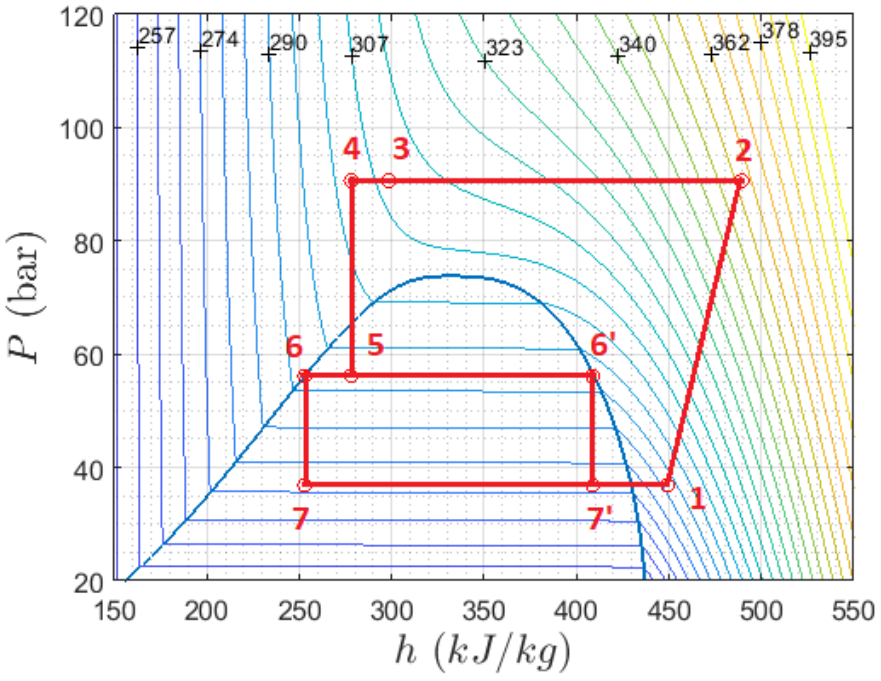

Fig. 2. P-h diagram of transcritical CO_2 heat pump

The CO_2 heat pump COP is calculated by the following relation:

$$COP = \frac{Q_h}{W_c} \tag{1}$$

where Q_h and W_c represent the heating capacity and the compressor power, respectively.

Q_h is calculated as follows:

$$Q_h = \dot{m}_g C_g (T_{go} - T_{gi}) \tag{2}$$

where $\dot{m}_g$and C_g denote mass flowrate and heat capacity, respectively, of the thermal fluid circulating in the gas cooler. T_{go} and T_{gi} are the outlet and inlet temperatures of the thermal fluid.

Similarly the combined COP for heating and cooling is determined by adding the cooling capacity Q_c to the numerator of equation 1.

Q_c is calculated as follows:

$$Q_c = \dot{m}_e C_e (T_{ei} - T_{eo}) \tag{3}$$

where $\dot{m}_e$and C_e denote mass flowrate and heat capacity, respectively, of the thermal fluid circulating in the evaporator. T_{eo} and T_{ei} are the outlet and inlet temperatures of the thermal fluid.

The root-sum-square method was applied for calculating uncertainties of measured variables as follows

$$\varepsilon_v = \sqrt{\sum_{i=1}^{k} \left(\frac{\partial v}{\partial \alpha_i} \varepsilon_{\alpha_i}\right)^2} \tag{4}$$

where v denotes the analyzed variable. α_i denotes the variable affecting v. ε_v and ε_{α_i} denote the uncertainties of v and α_i, respectively. This method is utilized for calculating uncertainties of measured variables in Equations 1 and 2. Uncertainty of COP (ε_{COP}) is calculated by:

$$\varepsilon_{COP} = \sqrt{\left(\frac{\partial COP}{\partial Q_h} \varepsilon_{Q_h}\right)^2 + \left(\frac{\partial COP}{\partial W_c} \varepsilon_{W_c}\right)^2} \tag{5}$$

where ε_{Q_h} and ε_{W_c} represent the uncertainties of Q_h and W_c, respectively. ε_{COP} is calculated by:

$$\varepsilon_{COP} = \sqrt{\left(\frac{\partial Q_h}{\partial \dot{m}_g} \varepsilon_{\dot{m}_g}\right)^2 + \left(\frac{\partial Q_h}{\partial T_{gi}} \varepsilon_{T_{gi}}\right)^2 + \left(\frac{\partial Q_h}{\partial T_{go}} \varepsilon_{T_{go}}\right)^2} \tag{6}$$

where $\varepsilon_{\dot{m}_g}$, $\varepsilon_{T_{gi}}$, and $\varepsilon_{T_{go}}$, denote the uncertainties of $\dot{m}_g$, T_{gi} , and T_{go}, respectively. Using measured data, ε_{COP} could be determined by Equations 1 to 6. Calculations shows that the maximum ε_{COP} is 3.92%.

3. Experimental Results and Discussion

The prototype previously described has been operated in order to assess its performances and study the effect of some governing parameters such as: discharge pressure, compressor speed, heat source and sink temperatures. Experimental results are presented hereafter.

3.1. Discharge pressure effect

The effects of the discharge pressure upon the key parameters characterizing the transcritical CO_2 heat-pump system are illustrated in Figures 3–5. The other influencing parameters are kept constant.

As shown in Figure 3, upon increasing the discharge pressure, the CO_2 mass flowrate gradually decreases. This results from the regulation of the discharge pressure by adjusting the EEV opening. If the EEV opening is reduced, the mass flowrate of CO_2 flowing through EEV decreases, leading to an excessive accumulation of CO_2 in the gas cooler. As a result, the discharge pressure and temperature increase and consequently, the heat generated at the gas cooler increases as displayed in Figure 4. Since the water temperature at the outlet of the gas cooler is regulated by the water flowrate to keep it close to a setpoint, the water flowrate is adjusted automatically as the discharge pressure increases by a PID that controls the pump's speed.

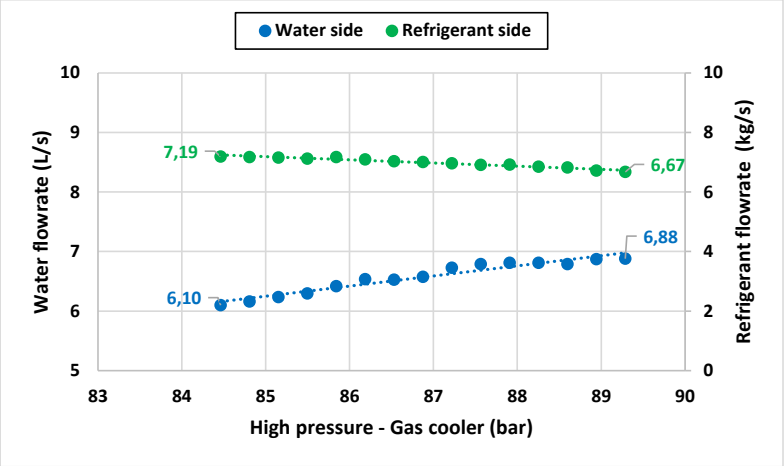

Fig. 3. Effect of discharge pressure on flowrates

Figure 4 displays the heating-cooling output and the compressor power demand as a function of the discharge pressure. It observed that an increase of discharge pressure results in a higher heating and cooling capacities. As the EEV closes, the discharge pressure increases, and the suction pressure decreases. Consequently, the discharge temperature is higher, and the evaporating temperature is lower. Thus, water flowrates increase in both the gas cooler and the evaporator to keep the pre-set temperatures at the exists constant. This explains the augmentation of the heating and cooling capacities. Upon increasing the discharge pressure, the specific work of the compressor increases significantly due to the increase of the compression ratio. However, the CO_2 mass flowrate decreases with the increase of the discharge pressure. It is important to mention that the influence of the specific work is much larger than that of the CO_2 mass flowrate, hence, the cross effect of the two factors lead to the increase of the power demand of the compressor.

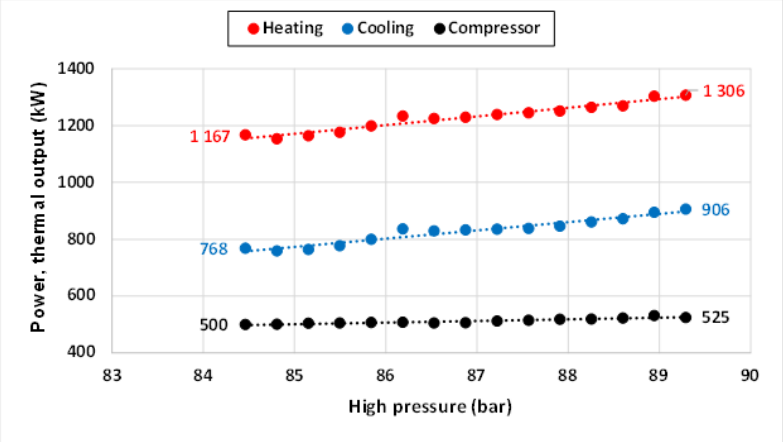

Fig. 4. Effect of discharge pressure on HP thermal outputs and power demand (HP: high pressure)

Figure 5 shows that with the increase of the discharge pressure, the COP rises steadily. Since the discharge pressures tested do not exceed 90 bar, it is unlikely to reach the optimum discharge pressure for which the COP is at its maximum. Based on the previous analysis, the power consumption increases monotonously with the increase of the discharge pressure.

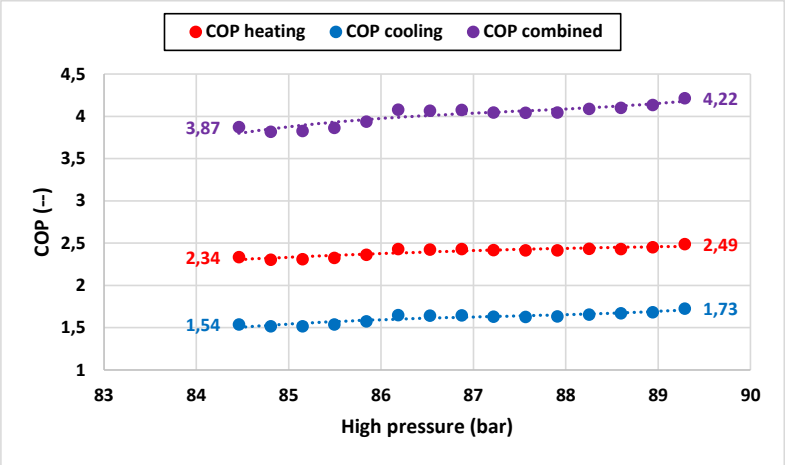

Fig. 5. Effect of discharge pressure on HP performance

3.2. Effect of compressor speed

Figure 6 presents the compressor power demand for different rotational speed: 2000 to 4200 rpm. As the compressor speed increases, the EEV opens to maintain the discharge pressure constant. Thus, the refrigerant flowrate increases as well as the flowrate of water since more thermal energy must be evacuated.

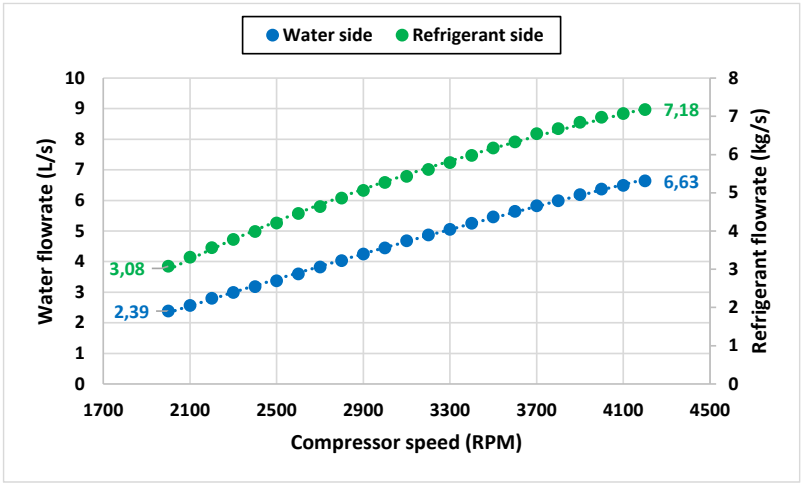

Fig. 6. Effect of compressor speed on flowrates

Indeed, Figure 7 shows that the heating output through the gas cooler increases as the compressor's speed evolves. It is worth mentioning that the decrease of the compressor speed reduces substantially the compressor power demand. For example, when the compressor speed drops from 4200 to 2000 rpm, the power demand is reduced by 57%.

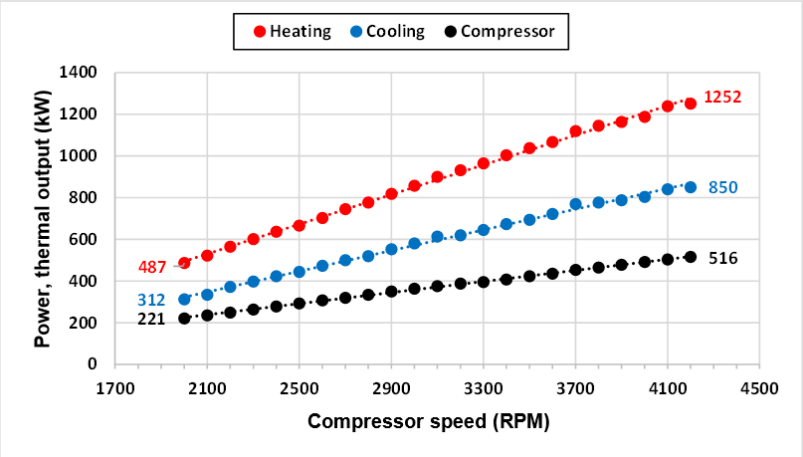

Fig. 7. Effect of compressor speed on HP thermal outputs and power demand

It is important to point that the influence of the compressor speed on the COP is not pronounced namely for speeds exceeding 3300 rpm as displayed in Figure 8. Indeed, the performance decreases by only 12% when the compressor speed drops from 4200 to 2000 rpm. This finding is important as it has an important impact for demand response applications for which the compressor speed variation is an advantage.

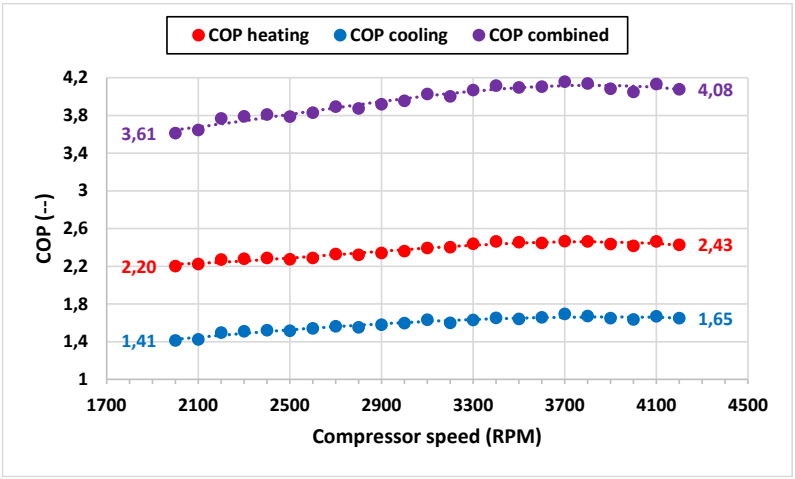

Fig. 8. Effect of compressor speed on HP performance

3.3. Heat source temperature effect

Heat source temperature is represented by the inlet water temperature at the evaporator. This parameter has been varied from 12°C to 20°C while the temperatures at the inlet and outlet of the gas cooler have been maintained constant at 20°C and 60°C respectively. The compressor speed was set at 4200 rpm and the high pressure was fixed at 86.2 bar.

Figure 9 displays that an increase in the heat source temperature results in an increase of the flowrates on both sides of the gas cooler. The increase of the refrigerant flowrate is due to an enhancement of the evaporating kinetic as more heat is supplied to the evaporator even though the compressor speed is kept constant. Since more heat is absorbed by the evaporator, it is expected that more heat will be released at the gas cooler (Fig. 9). In this case, the water flowrate will increase to maintain the water outlet temperature at the set-point of 60°C.

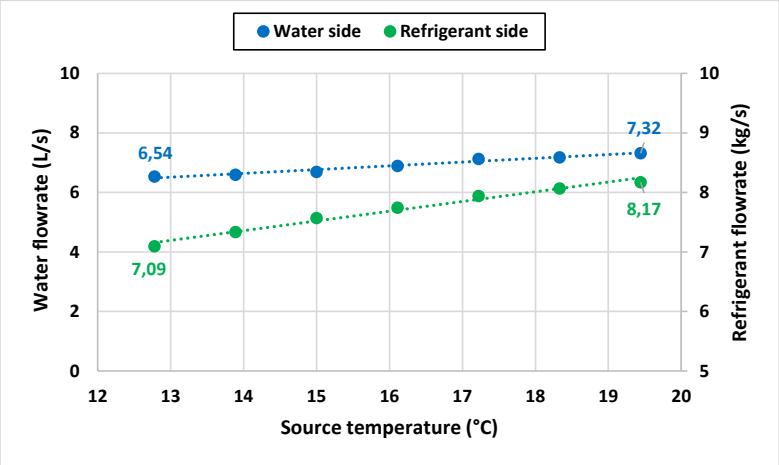

Fig. 9. Effect of heat source temperature on flowrates

Figure 10 displays the impact of heat source temperature on thermal outputs and compressor power demand. The increase of the heat source temperature at the evaporator increases the heat adsorbed and rejected by the heat pump as mentioned before. The power demand of the compressor rises as well because of an increase of the refrigerant flowrate occurs due to an enhancement of the vaporizing process in the evaporator. As a consequence, the performance of the heat pump is improved as shown in Figure 11.

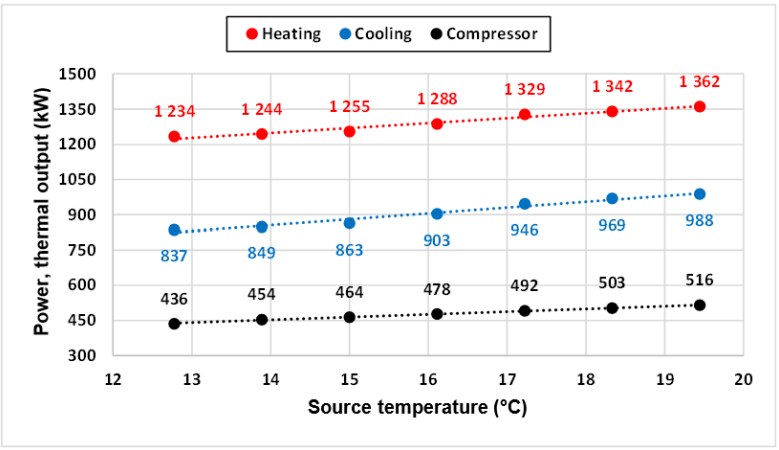

Fig. 10. Effect of heat source temperature on HP thermal outputs and power demand

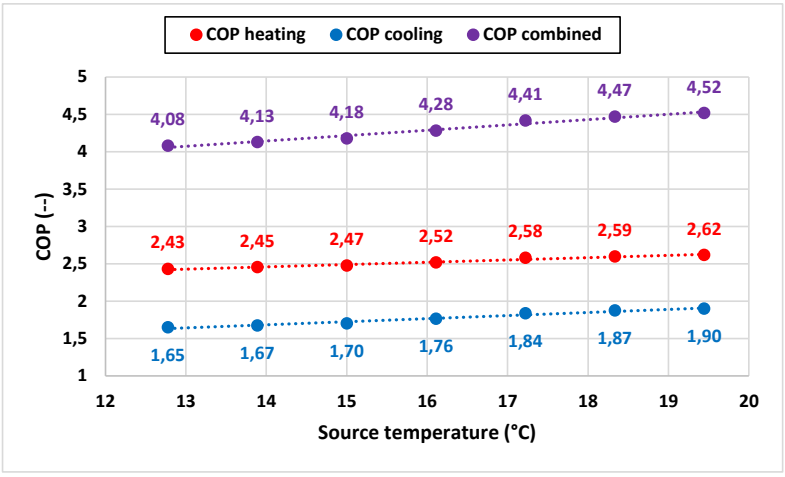

Fig. 11. Effect of heat source temperature on HP performance

3.4. Heat sink temperature effect

Figure 12 displays the variation of the COP for both heating and cooling as a function of the water temperatures at the inlet and outlet of the gas cooler for different discharge pressures. The compressor speed and the heat source temperature are kept constant at 3500 rpm and 12 °C, respectively.

Results show that for a constant outlet temperature at the gas cooler when the inlet temperature increases, the performance deteriorates. Since an increase in the inlet temperature results in an increase of the CO_2 temperature at the outlet of the gas cooler, the heat absorbed at the evaporator is less and consequently, the thermal output decreases.

On the other hand, when the inlet temperature is kept constant, any reduction in the outlet temperature will lead to an increase of the COP. In fact, the water flowrate through the gas cooler is higher when the outlet temperature is reduced.

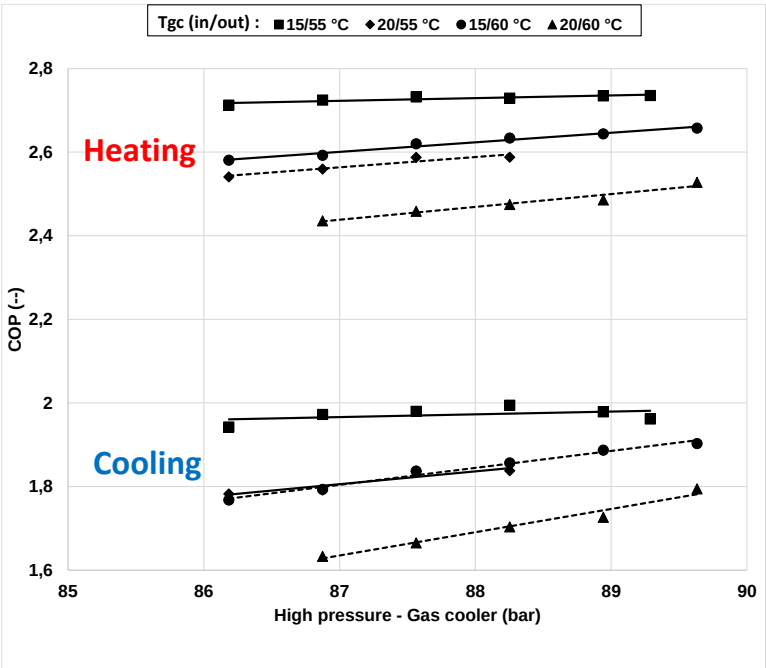

Fig. 12. Effect of gas cooler inlet outlet temperatures on HP performance (3500 rpm and T_{source} = 12°C)

4. Conclusion

A transcritical CO_2 heat pump has been built at the pilot-scale to demonstrate the potential of such a technology to provide heating and cooling to large buildings. The heat pump is composed of an open single screw compressor, shell and tube heat exchangers (flooded at the evaporator), expansion valves, a flash tank and a copper brazed plates internal heat exchanger. The water loop system includes thermal storage tanks that decouple the thermal load from the CO2 heat pump and enable performance enhancement. Detailed information about the main components is summarized in Table 1.

The influences of the discharge pressure, compressor speed, and heat source and sink temperatures on the main performances of the system have been quantified in detail and discussed. The main results may be summarized as follows:

- Both heating and cooling COPs are increasing as a function of the discharge pressure, compressor speed, and heat source / sink temperatures.
- The maximum heating and cooling power capacities are 1.362 and 0.988 MW, respectively.
- The maximum COP values are 2.75 and 2 for heating and cooling, respectively, leading to a maximum combined COP of 4.75. (Real COP measured based on heat outputs on the water sides).

This technology appears as a valuable way for the decarbonization and efficient electrification of large commercial or residential building, Future works include the detailed investigation of the water storage tank and more particularly its optimal design to manage the thermocline.

Acknowledgements

The authors would like to thank the engineering team of Vilter and Ceptek for their technical support and the technical staff of Hydro Quebec for the build-up and operation of the industrial prototype.

References

[1] Delmastro C, Heat pumps – more efforts needed, Tracking report of International Energy Agency, 2022.
[2] Rosenow J, Gibb D, Nowak T, Lowes R. Heating up the global heat pump market. *Nature Energy* 2022.
[3] Gaur AS, Fitiwi DZ, Curtis J. Heat pumps and our low-carbon future: A comprehensive review. *Energy Res Soc Sci* 2021; **71**:101764.
[4] Wang Y, Wang J, He W. Development of efficient, flexible and affordable heat pumps for supporting heat and power decarbonisation in the UK and beyond: Review and perspectives. *Renew Sust Energy Rev* 2022; **154**: 111747.
[5] Ni L, Dong J, Yao Y, Shen C, Qv D, Zhang X. A review of heat pump systems for heating and cooling of buildings in China in the last decade. *Renew Energy* 2015;**84**:30-45.
[6] Volkova A, Koduvere H, Pieper H. Large-scale heat pumps for district heating systems in the Baltics: Potential and impact. *Renew Sust Energy Rev* 2022; **167**: 112749.
[7] Popovski E , Aydemir A, Fleiter T, Bellstadt D, Büchele R, Steinbach J. The role and costs of large-scale heat pumps in decarbonising existing district heating networks - A case study for the city of Herten in Germany. *Energy* 2019; **180**: 918-933.
[8] Bach B, Werling J, Ommen T, Munster M, Morales JM, Elmegaard B. Integration of large-scale heat pumps in the district heating systems of Greater Copenhagen. *Energy* 2016; **107** : 321-334.
[9] David A, Vad Mathiesen B, Averfalk H, Werner S, Lund H. Heat Roadmap Europe: Large-Scale Electric Heat Pumps in District Heating Systems. *Energies* 2017; **10** : 578.
[10] Schlosser F, Jesper M, Vogelsang J, Walmsley TG, Arpagaus C, Hessekbach J. Large-scale heat pumps: Applications, performance, economic feasibility and industrial integration. *Renew Sust Energy Rev* 2020; **133**: 110219.
[11] Jesper M, Schlosser F, Pag F, Walmsley TG, Schmitt B, Vajen K. Large-scale heat pumps: Uptake and performance modelling of market-available devices. *Renew Sust Energy Rev* 2021; **137**: 110646.
[12] Wang Y, Wang Z, Li M, Chen T, Wang Z. An optimal matching strategy for screw compressor for heat pump applications. *Appl Therm Eng* 2018; **132**: 333-340.
[13] Song Y, Cui C, Yin X, Cao F. Advanced development and application of transcritical CO_2 refrigeration and heat pump technology—A review. *Energy Reports* 2022; **8**: 7840-7869.
[14] Osterman E, Stritih U. Review on compression heat pump systems with thermal energy storage for heating and cooling of buildings. *J Energy Storage* 2021; **39**:102569.
[15] Liu F, Zhu W, Cai Y. Experimental study of a dual-mode CO_2 heat pump system with thermal storage. *Energy Proc* 2017; **105** : 4078–4083.
[16] Alkhwildi A, Elhashmi R, Chiasson A. Parametric modeling and simulation of Low temperature energy storage for cold-climate multi-family residences using a geothermal heat pump system with integrated phase change material storage tank. *Geothermics* 2020; **86** : 101864.